

characteristics of 353 patients. *Arch Neurol*, 62; 925-930, 2005

12) Kemp, P.M., Holmes, C., Hoffmann, S.M., et al.: Alzheimer's disease: differences in technetium-99m HMPAO SPECT scan findings between early onset and late onset dementia. *J Neurol Neurosurg Psychiatry*, 74; 715-719, 2003

13) Koss, E., Edland, S., Fillenbaum, G., et al.: Clinical neuropsychological differences between patients with earlier and later onset of Alzheimer's disease: A CERAD analysis, part XII. *Neurology*, 46; 136-141, 1996

14) Kowalska, A., Asada, T., Arima, K., et al.: Genetic analysis in patients with familial and sporadic frontotemporal dementia: two tau mutations in only familial cases and no association with apolipoprotein epsilon 4. *Dement Geriatr Cogn Disord*, 12; 387-392, 2001

15) Lampe, T.H., Bird, T.D., Nochlin, D., et al.: Phenotype of chromosome 14-linked familial Alzheimer's disease is a large kindred. *Ann Neurol*, 36; 368-378, 1994

16) McKeith, I.G., Fairbairn, A., Perry, R.H., et al.: Neuroleptic sensitivity in patients with senile dementia of Lewy body type. *BMJ*, 305; 673-678, 1992

17) McKeith, I.G., Perry, E.K., Perry, R.H., et al.: People at the second dementia with Lewy body international workshop: diagnosis and treatment. Consortium on dementia with Lewy bodies. *Neurology*, 53; 902-905, 1999

18) McKeith, I.G., Dickson, D.W., Lowe, J., et al.: Diagnosis and management of dementia with Lewy bodies: third report of the DLB consortium. *Neurology*, 65; 1863-1872, 2005

19) McKeith, I.G.: Dementia with Lewy bodies: a clinical overview. *Dementia*, 3rd ed. (ed. by Burns, A., O'Brien, J., et al). Hodder Arnold, New York, p. 603-614, 2005

20) Mendez, M.F., Cummings, J.L.: Dementia: significance, definition, and epidemiology. *Dementia*, 3rd ed. Butterworth Heinemann, Philadelphia, p. 1-12, 2003

21) Mendez, M.F., Cummings, J.L.: Frontotemporal dementia and the asymmetric cortical atrophies. *Dementia*, 3rd ed. Butterworth Heinemann, Philadel-

phia, p. 179-233, 2003

22) Neary, D., Snowden, J.S., Northen, B., et al.: Frontotemporal lobar degeneration: a consensus on clinical diagnostic criteria. *Neurology*, 51; 1546-1554, 1998

23) Neumann, M., Sampathu, D.M., Kwong, L.K., et al.: Ubiquitinated TDP-43 in frontotemporal lobar degeneration and amyotrophic lateral sclerosis. *Science*, 314; 130-133, 2006

24) Newens, A.J., Foster, D., Kay, D., et al.: Clinically diagnosed presenile dementia of Alzheimer type in the Northern Health Region. *Psychol Med*, 23; 631-644, 1993

25) Papka, M., Rubio, A., Schiffer, R.: A review of Lewy body disease, an emerging concept of cortical dementia. *J Neuropsychiatry Clin Neurosci*, 10; 267-279, 1998

26) Perry, R.H., Irving, D., Blessed, G., et al.: Clinically and neuropathologically distinct form of dementia in the elderly. *Lancet*, i; 166, 1989

27) Plassman, B.L., Breitner, J.C.: Recent advances in the genetics of Alzheimer's disease and vascular dementia with an emphasis on gene-environmental interactions. *J Am Geriatr Soc*, 44; 1242-1250, 1996

28) Rogaev, E., Sherrington, R., Liang, Y.: Familial Alzheimer's disease in kindreds with missense mutation in a gene on chromosome 1 related to the Alzheimer's disease type 3 gene. *Nature*, 376; 600-602, 1995

29) Ropper, A.H., Williams, R.S.: Relationship between plaque, tangles, and dementia in Down syndrome. *Neurology*, 30; 639-644, 1980

30) Roses, A.D.: Apolipoprotein E affects the role of Alzheimer disease expression: beta-amyloid burden is a secondary consequence dependent on APOE genotype and duration of disease. *Neuropathol Exp Neurol*, 53; 429-437, 1994

31) Schellenberg, G.D.: Genetic dissection of Alzheimer disease. *Proc Natl Acad Sci USA*, 92; 8552-8559, 1995

32) Weiner, M.F., Risser, R.C., Cullum, C.M., et al.: Alzheimer's disease and its Lewy body variant: a clinical analysis of postmortem verified cases. *Am J Psychiatry*, 153; 1269-1273, 1996

- 33) Zhukareva, V., Vogelsberg-Ragaglia, V., Van Deerlin, V.M., et al.: Loss of brain tau defines novel sporadic and familial tauopathies with frontotemporal dementia. *Ann Neurol*, 49: 165-175, 2001.
- 

## Young-onset Dementia : An Unresolved Challenge

Takashi ASADA

*Department of Neuropsychiatry, Institute of Clinical Medicine, University of Tsukuba*

Younger people with dementia present a unique challenge to modern Japanese society and those individuals who care for them. Although illnesses causing dementia occur much less commonly in younger than older people, it was estimated that there were about 30,000 affected younger people in 1995 in Japan. For younger people with dementia, effects on families, the presence of dependent young children, and the economic implications are particular challenges.

In this article, firstly, epidemiological findings regarding illnesses causing dementia in younger people were described. Secondly, the three major degenerative dementia forms that often develop in presenescence were reviewed.

Thirdly, the issue of service planning for such cases was discussed.

<Author's abstract>

<Key words>: presenile dementia, epidemiology, Alzheimer, frontotemporal dementia, dementia with Lewy bodies>

---

# A preliminary open-label study of 5-HT<sub>1A</sub> partial agonist tandospirone for behavioural and psychological symptoms associated with dementia



Shinji Sato<sup>1</sup>, Katsuyoshi Mizukami<sup>2</sup> and Takashi Asada<sup>2</sup>

<sup>1</sup> Department of Psychiatry, Tsukuba Memorial Hospital, Tsukuba, Japan

<sup>2</sup> Department of Neuropsychiatry, Institute of Clinical Medicine, Tsukuba University, Tsukuba, Japan

## Abstract

The aim of this study was to assess the efficacy and safety of tandospirone, a 5-HT<sub>1A</sub> partial agonist, for treatment of behavioural and psychological symptoms of dementia (BPSD). Thirteen outpatients with DSM-IV diagnosis of Alzheimer's type or vascular dementia were enrolled in this study. Their BPSD and cognitive functions were evaluated with the Neuropsychiatric Inventory (NPI) and Mini-Mental State Examination, respectively, for an 8-wk period of treatment. The maximum benefit of tandospirone was achieved at a mean dose of 19.6 mg/d. There were significant improvements in the NPI subscores for delusion, agitation, depression, anxiety, and irritability at 2 or 4 wk after the start of administration of tandospirone. No patients experienced severe adverse effects. The results suggest that tandospirone was effective at improving BPSD symptoms and well-tolerated in elderly demented patients.

Received 23 March 2006; Reviewed 11 April 2006; Revised 9 May 2006; Accepted 13 May 2006;

First published online 3 July 2006

**Key words:** Behavioural and psychological symptoms of dementia, dementia, tandospirone, 5-HT<sub>1A</sub> agonist.

## Introduction

The International Psychiatric Association defines Behavioral and Psychological Symptoms of Dementia (BPSD) as non-cognitive symptoms such as behaviour (e.g. agitation, aggression, wandering, screaming) and psychiatric disturbances (e.g. hallucination, delusion, depression, anxiety, insomnia). In a previous study, BPSD was observed in 20–80% of patients with dementia (Lawlor, 2004). BPSD often could have a negative impact on patients' daily activities, and especially on caregivers' quality of life (Lawlor, 2004). Although non-pharmacological interventions should be a first-line treatment for BPSD, severe BPSD often needs to be managed with psychotropic agents, especially atypical neuroleptics such as risperidone, olanzapine, and quetiapine (Lawlor, 2004). Recently, increased mortality has been reported in elderly patients with dementia using atypical antipsychotics (Food and

Drug Administration, 2005) as well as conventional antipsychotic medications (Wang et al., 2005). Thus, it is crucial to develop a safer treatment for BPSD in demented patients.

Tandospirone citrate, a 5-HT<sub>1A</sub> partial agonist produced in Japan, is an anxiolytic azapirone, and has shown anti-anxiety effects as well as antidepressant effects with remarkable tolerability (Murasaki et al., 1992). Although there have been only a few reports regarding the effects of tandospirone on BPSD, buspirone, a 5-HT<sub>1A</sub> partial agonist like tandospirone, has been reported to be effective at managing agitation or aggressive behaviour, and to be well tolerated in patients with dementia (Cantillon et al., 1996). Here, we report the usefulness of tandospirone for treating various behavioural and psychological symptoms of dementia.

## Method

### Subjects

Thirteen subjects were recruited from the outpatient clinic of Tsukuba Central Hospital between April 2003 and April 2004. All had either Alzheimer's disease

Address for correspondence: K. Mizukami, M.D., Ph.D., Department of Psychiatry, Institute of Clinical Medicine, University of Tsukuba, 1-1-1 Tennodai, Tsukuba, Ibaraki 305-8575, Japan.  
Tel.: (+81)29-853-3210 Fax: (+81)29-853-3182  
E-mail: mizukami@md.tsukuba.ac.jp

**Table 1.** Mean (s.d.) of Neuropsychiatric Inventory (NPI) scores at each time-point with tandospirone ( $n = 13$ )

Subscale	Baseline	2 wk after	4 wk after	6 wk after	8 wk after
Delusion	5.2 (4.9)	3.9 (3.8)	3.1 (3.0)*	3.5 (2.8)	3.5 (2.8)
Hallucination	0.9 (3.3)	0.9 (3.3)	0.1 (0.3)	0.7 (2.2)	0.7 (2.2)
Agitation/Aggression	6.6 (4.4)	4.5 (3.5)*	3.4 (2.6)**	3.2 (2.5)**	3.2 (2.5)**
Depression/Dysphoria	4.2 (5.3)	3.4 (4.1)	2.2 (2.7)*	2.2 (2.8)*	2.0 (2.7)*
Anxiety	5.8 (5.2)	4.2 (3.9)*	3.2 (2.8)*	2.9 (2.6)*	2.5 (2.0)*
Euphoria/Elation	0.0 (0.0)	0.0 (0.0)	0.0 (0.0)	0.0 (0.0)	0.0 (0.0)
Apathy/Indifference	4.9 (4.1)	4.6 (3.9)	4.6 (3.9)	4.6 (3.9)	4.6 (3.9)
Disinhibition	1.5 (2.7)	1.5 (2.7)	0.8 (1.3)	0.8 (1.3)	0.9 (1.4)
Irritability/Lability	6.5 (4.5)	4.4 (4.0)*	2.7 (2.8)**	2.6 (2.9)**	2.6 (2.9)**
Aberrant motor behaviour	5.2 (4.6)	4.8 (4.6)	3.9 (4.4)	3.9 (4.4)	3.9 (4.4)

NPI subscale scores at each time-point were compared to baseline scores using the Wilcoxon signed-rank test.

\*  $p < 0.05$ , \*\*  $p < 0.01$ .

(AD) or vascular dementia (VD), according to DSM-IV (APA, 1994) diagnostic criteria, and exhibited one or more BPSD symptoms that had been unmanageable with non-pharmacotherapy for at least 1 month. All patients and their caregivers provided written informed consent for study participation; if a patient lacked the ability to give consent, we obtained it from his/her caregiver. The patients underwent physical, neurological, and laboratory examinations as well as brain magnetic resonance imaging or brain computed tomography. If they had a serious physical illness or a past history of mental or neurological disorders, they were excluded from the study.

#### Study design

The trial was an open-label, 8-wk study. The Mini-Mental State Examination (MMSE) and Clinical Global Impression (CGI) Rating Scale were used to assess the severity of cognitive deficits at baseline, and to evaluate the clinical improvements at 8 wk. The frequency and severity of BPSD were assessed according to the Neuropsychiatric Inventory (NPI; Cummings et al., 1994) at baseline and 2, 4, 6, and 8 wk after the start of tandospirone administration. Initially, the administration of tandospirone started at 10 mg/d, divided into morning and evening doses. If the efficacy was deemed insufficient, the daily dose was increased weekly by 5 mg/d to a maximum dose of 30 mg/d. The maximum effective and tolerated dose was determined based on clinical judgment and NPI scores. Ten patients in this study were receiving other medications (tiapride 3, donepezil 4, risperidone 2, and mianserine 2) at the study's start. These medications were continued at the same dose. We did not add or change any psychotropic medications during the

investigation. Changes in the NPI scores were analysed by means of the Wilcoxon signed-rank test.

#### Results

All patients completed this trial. Their mean age was  $76.7 \pm 7.8$  (range 67–93) yr, and seven (53.8%) of the 13 patients were male. Among the patients analysed, six (46.2%) had AD and seven (53.8%) had VD. Their baseline MMSE score was  $13.9 \pm 6.5$  (range 0–22). The maximum benefit of tandospirone was achieved at  $19.6 \pm 8.0$  mg/d (range 10–30). No serious adverse effects were observed during the study. The efficacy evaluations at each time-point are shown in Table 1. At 8 wk, scores for agitation/aggression, anxiety, irritability/lability, and depression/dysphoria significantly improved. These symptoms, except for depression/dysphoria, had already improved at 2 wk after the treatment with tandospirone, while the depression/dysphoria score significantly improved 4 wk after the treatments start. For evaluation of CGI, clinical improvements of the BPSD were observed in 10 (77%) of the 13 patients (6 very much improved, 1 much improved, 3 minimally improved, 2 no change, 1 minimally worse).

Despite study design limitation, this open-label pilot trial suggests that moderate doses of tandospirone (mean dose 19.6 mg/d) significantly reduced the severity and frequency of BPSD, including psychological symptoms such as depression, anxiety, and irritability/lability, as well as behavioural symptoms such as agitation and aggression. In addition, approximately 70% of the subjects showed clinical improvements in the symptoms evaluated by CGI. No patients showed serious adverse effects such as extrapyramidal symptoms and drowsiness, which

are often observed in patients taking neuroleptics and benzodiazepine. Collectively, our study suggests that tandospirone is an effective and well-tolerated treatment for BPSD.

### Discussion

Recently, the effects of buspirone, a 5-HT<sub>1A</sub> partial agonist like tandospirone, on aggression and agitation in demented patients have been reported (Cantillon et al., 1996). Lai et al. (2003) have reported that the 5-HT<sub>1A</sub> receptor density in brains of AD patients correlates negatively with the maladaptive behaviour of aggression. It has also been reported that in a case study, tandospirone improved aggression in four out of seven demented patients (Yamane, 2001). The present study suggests that tandospirone is effective for aggression and agitation in patients with dementia, presumably due to improvements in serotonergic dysfunction in the brain. We also observed the effects of tandospirone on depression and anxiety symptoms of patients with dementia in this study. A double-blind study comparing tandospirone and diazepam for the treatment of neurosis demonstrated that tandospirone has shown anti-anxiety effects similar to diazepam, and also that tandospirone had anti-depressant effects (Murasaki et al., 1992). In a prior study of nine demented patients with depressive symptoms, 15 mg/d tandospirone manifested an effect on depressive symptoms (Masuda et al., 2002). The results of our study are consistent with those of these prior studies. In addition, our study showed improvements in agitation/aggression, anxiety, and irritability/lability at 2 wk, thus indicating that tandospirone takes effect relatively soon after commencing treatment. Recently, Sumiyoshi et al. (2001) reported that tandospirone is useful for improving cognitive performance in patients with schizophrenia. Although it remains to be determined if tandospirone improves cognitive function in patients with dementia, it is reasonable to suppose that tandospirone is also safe with respect to cognitive function, since neuroleptics often induce aggravation of cognitive function in patients with dementia.

In the present study, tandospirone showed a lack of severe adverse effects, and was effective for various BPSD; thus, tandospirone is a promising medicine for safely managing BPSD.

### Acknowledgements

None.

### Statement of Interest

None.

### References

- APA (1994). *Diagnostic and Statistical Manual of Mental Disorders* (4th edn). Washington, DC: American Psychiatric Association.
- Cantillon M, Brunswick R, Molina D, Bahro M (1996). Buspirone vs. haloperidol: a double-blind trial for agitation in a nursing home population with Alzheimer's disease. *American Journal of Geriatric Psychiatry* 4, 263-267.
- Cummings JL, Mega M, Gray K, Rosenberg-Thompson S, Carusi DA, Gornbein J (1994). The Neuropsychiatric Inventory: comprehensive assessment of psychopathology in dementia. *Neurology* 44, 2308-2314.
- Food and Drug Administration (2005). FDA Public Health Advisory: deaths with Antipsychotics in Elderly Patients with Behavioral Disturbances, 11 April 2005. (<http://www.fda.gov/cder/drug/advisory/antipsychotic.htm>). Accessed 21 July 2005.
- Lai MK, Tsang SW, Francis PT, Esiri MM, Keene J, Hope T (2003). Reduced serotonin 5-HT<sub>1A</sub> receptor binding in the temporal cortex correlates with aggressive behavior in Alzheimer's disease. *Brain Research* 974, 82-87.
- Lawlor BA (2004). Behavioral and psychological symptoms in dementia: the role of atypical antipsychotics. *Journal of Clinical Psychiatry* 65 (Suppl. 11), 5-10.
- Masuda Y, Akagawa Y, Hishikawa Y (2002). Effect of serotonin 1A agonist tandospirone on depression symptoms in senile patients with dementia. *Human Psychopharmacology: Clinical and Experimental* 17, 191-193.
- Murasaki M, Mori A, Endo S, Takemasa K, Hasegawa K, Kamishima K (1992). Efficacy of a new anxiolytic, tandospirone (SM-3997) on neurosis [in Japanese]. *Clinical Evaluation* 20, 295-329.
- Sumiyoshi T, Matsui M, Nohara S, Yamashita I, Kurachi M, Sumiyoshi C, Jayathilake K, Meltzer HY (2001). Enhancement of cognitive performance in schizophrenia by addition of tandospirone to neuroleptic treatment. *American Journal of Psychiatry* 158, 1722-1725.
- Wang PS, Schneeweiss S, Avorn J, Fischer MA, Mogun H, Solomon DH (2005). Risk of death in elderly users of conventional vs. atypical antipsychotic medications. *New England Journal of Medicine* 353, 2335-2341.
- Yamane H (2001). Tandospirone clinical adaptation of dementia with aggression [in Japanese]. *Japanese Journal of Psychiatric Treatment* 16, 169-172.

## Relationship between diffusion tensor imaging and brain morphology in patients with myotonic dystrophy

Miho Ota<sup>a</sup>, Noriko Sato<sup>a,\*</sup>, Yasushi Ohya<sup>c</sup>, Yoshitsugu Aoki<sup>c</sup>,  
Katsuyoshi Mizukami<sup>b</sup>, Takeyuki Mori<sup>a</sup>, Takashi Asada<sup>b</sup>

<sup>a</sup> Department of Radiology, National Center Hospital for Mental, Nervous and Muscular Disorders, National Center of Neurology and Psychiatry, 4-1-1 Ogawahigashi, Kodaira, Tokyo 187-8551, Japan

<sup>b</sup> Department of Neuropsychiatry, Institute of Clinical Medicine, University of Tsukuba, 1-1-1 Tennoudai, Tsukuba, Ibaraki 305-8575, Japan

<sup>c</sup> Department of Neurology, National Center Hospital for Mental, Nervous and Muscular Disorders, National Center of Neurology and Psychiatry, 4-1-1 Ogawahigashi, Kodaira, Tokyo 187-8551, Japan

Received 14 July 2006; received in revised form 21 August 2006; accepted 29 August 2006

### Abstract

Myotonic dystrophy type 1 (MyD) is a common inherited neuromuscular disorder. In addition to neuromuscular symptoms, many MyD patients show central nervous system neuropathology. This study evaluated whether MyD patients display diffusion tensor (DT) abnormalities associated with regional cortical atrophy and clinical features. Three-dimensional T1-weighted and DT magnetic resonance images of the brain were obtained in 11 MyD patients and 13 age- and sex-matched healthy subjects. Fractional anisotropy (FA) and mean diffusivity (MD) values were calculated in corpus callosum subregions with DT imaging (DTI) along with volumetric changes, and correlations with clinical features were examined. Differences between MyD patients and healthy subjects were analyzed statistically. Significantly lower FA and higher MD values were found in the genu, rostral body, anterior midbody, posterior midbody and splenium in MyD patients than in control subjects ( $p < 0.05$ , corrected; lower FA in the splenium was at a trend level). These corpus callosum subregions were the areas connected to cortical areas where significantly lower volumes were found in MyD patients. No significant decrease in volumes was noted in the parietal cortex, where connecting fibers pass through the isthmus in which DTI abnormalities were not detected in MyD patients. Significant negative correlations to volumes of frontal areas were noted, particularly bilateral motor areas, with cytosine thymine guanine (CTG) triplet expansion. DTI results in corpus callosum may reflect morphological changes in the connecting cortical areas of MyD patients.

© 2006 Elsevier Ireland Ltd. All rights reserved.

**Keywords:** Myotonic dystrophy; Fractional anisotropy; Mean diffusivity; Voxel-based morphometry; CTG repeat

Myotonic dystrophy (MyD) is a hereditary disease characterized by muscular atrophy and myotonia associated with various systematic abnormalities, including some in the central nervous system [11]. MyD patients display cognitive disorder, personality change and hypersomnia. This progressive autosomal dominant, multisystemic disease is characterized by an unstable triplet cytosine thymine guanine (CTG) repeat on chromosome 19, which appears to be excessively amplified [8].

Previous magnetic resonance imaging (MRI) studies of the brain have shown ventriculomegaly, scattered patches of increased signal in white matter, and cortical atrophy in

MyD patients [1,4]. Some pathological data concerning brain involvement in MyD have shown central nervous system neuropathology, cell loss in the cerebral cortex, neuronal inclusion bodies mostly in the thalamus, caudate and other brainstem nuclei, decreased myelin sheathing, and increased neurofibrillary tangles [11,18]. However, few studies have examined relationships between morphometric or microstructural changes of the brain and disease severity.

Diffusion tensor imaging (DTI) is a sophisticated MRI technique that reveals tissue microstructure [16,17], allows in vivo white matter tract imaging [2], and provides measures of both diffusivity (a measure of mean diffusivity (MD), averaged in all spatial directions) and fractional anisotropy (FA), a measure of the directionality of diffusion [22]. DTI analysis of cerebral white matter in MyD patients has been reported

\* Corresponding author. Tel.: +81 42 341 2711; fax: +81 42 346 2094.  
E-mail address: [snorko@ncnp.go.jp](mailto:snorko@ncnp.go.jp) (N. Sato).

previously [9,23], but scattered patches of increased signal in white matter made microstructural changes in manually plotted regions of interest (ROIs) difficult to discuss.

The corpus callosum (CC) displays heterotopic anteroposterior cortical connectivity. Furthermore, specific regions of the CC (i.e., genu, rostral body, anterior midbody, posterior midbody, isthmus and splenium) comprise fibers connecting hetero- and unimodally associated cortical regions [13,25]. The genu, rostral body, anterior midbody, posterior midbody, isthmus and splenium comprise fibers connecting caudal/orbital prefrontal areas and inferior premotor area, prefrontal area, frontal area and motor system, frontal area and motor system, parietal area, temporal and occipital areas, respectively, and the FA and MD values of CC subregions are linked to the associated regions [12,21]. Evaluation of normal-appearing white matter of the CC subregions could be used as a marker of the projection area, where ROIs are difficult to place.

This study performed DTI and voxel-based morphometry (VBM), which can be used to evaluate regional changes in brain volumes, to determine whether MyD patients have DT abnormalities associated with regional cortical atrophy. Furthermore, we also evaluated relationships between these MR data and various clinical features, such as CTG triplet expansion.

A total of 11 MyD patients (six men, five women; mean age,  $56.6 \pm 8.6$  years; mean duration of illness  $28.5 \pm 15.5$  years; mean age at onset,  $28.2 \pm 13.8$  years) and 13 sex- and age-matched healthy subjects (six men, seven women; mean age,  $56.3 \pm 12.5$  years) were examined. Patients with congenital MyD or any other neurological disease, and healthy subjects with neurological illness, head trauma, loss of consciousness or psychiatric disorder were excluded. Diagnosis was made based on family history, presence of myotonia on clinical examination and/or myotonic discharge on electromyographic examination. Diagnosis was confirmed by linkage analysis using DNA markers on chromosome 19 evaluated in all patients from leukocytes and showing abnormally numerous repeats of the CTG fragment. For clinical data, disease duration, age at onset and age at scan date were examined, in addition to repeats of CTG triplet expansion in each patient. All participants provided written informed consent, and the protocol was approved by the local ethics committee.

MR images were performed on a 1.0-T Magnetom Harmony system (Siemens, Erlangen, Germany). DTI was performed in the axial plane (echo time (TE)/repetition time (TR), 113/10,100 ms; field of view (FOV),  $230 \text{ mm} \times 230 \text{ mm}$ ; matrix,  $128 \times 128$ ; 40 continuous transverse slices; slice thickness 3 mm with no interslice gap). To enhance the signal-to-noise ratio, acquisition was repeated 5 times. Diffusion was measured along 12 non-collinear directions ( $(x, y, z) = [(1, 0, 0.5) (0, 0.5, 1) (0.5, 1, 0) (1, 0.5, 0) (0, 1, 0.5) (0.5, 0, 1) (1, 0, -0.5) (0, -0.5, 1) (-0.5, 1, 0) (1, -0.5, 0) (0, 1, -0.5) (-0.5, 0, 1)]$ ) with the use of a diffusion-weighted factor  $b$  in each direction for  $700 \text{ s/mm}^2$ , and one image was acquired without use of a diffusion gradient. The signal-to-noise ratio in the  $b=0$  image was roughly 30 in the central semioval. This was large enough to accurately estimate the parameters [14]. The DTI examination took approximately 11 min. High spatial-resolution, 3-dimensional (3D) T1-

weighted images of the brain were obtained for morphometric study. The 3D T1-weighted images were scanned in the sagittal plane (TE/TR, 3.93/2080 ms; flip angle,  $15^\circ$ ; effective slice thickness, 1.23 mm; slab thickness, 177 mm; matrix,  $208 \times 256$ ; FOV,  $256 \text{ mm} \times 315 \text{ mm}$ ; acquisition, 1) yielding 144 contiguous slices through the head. In addition to DTI and 3D T1-weighted images, conventional axial T2-weighted turbo spin echo images (TE/TR, 89/6580 ms; flip angle,  $180^\circ$ ; slice thickness, 5 mm; intersection gap, 0.4 mm; matrix,  $128 \times 128$ ; FOV,  $230 \text{ mm} \times 230 \text{ mm}$ ; acquisition, 1) and fluid attenuation inversion recovery images in an axial plane (TE/TR, 104/9100 ms; flip angle,  $150^\circ$ ; slice thickness, 3 mm; intersection gap, 0 mm; matrix,  $256 \times 256$ ; FOV,  $230 \text{ mm} \times 230 \text{ mm}$ ; acquisition, 1) were acquired to exclude cerebral vascular disease. On conventional MRI, no abnormal findings were detected in the brain except for cerebral atrophy and cerebral white matter signal abnormalities compatible with MyD in all patients.

Raw diffusion tensor data were transferred to a workstation and DTI data sets were analyzed using DtiStudio software (H. Jiang, S. Mori; Johns Hopkins University). Diffusion tensor parameters were calculated on a pixel-by-pixel basis, then FA, MD, and finally 3D fiber tracts were calculated. Fiber tractography was performed with a threshold value of fiber-tracking termination of FA = 0.2 and a trajectory angle of  $50^\circ$  [13]. In this study, we selected the range-designated tract fibers as the ROIs for the evaluation of FA and MD in the same manner as previously reported [21,25]. Six callosal subdivisions were defined at the midsagittal plane, with the CC being divided into the genu, rostral body, anterior midbody, posterior midbody, isthmus and splenium, from anterior to posterior. The anterior half included the genu, rostral body and anterior midbody. The line perpendicular to the axis at the anterior point on the inner convexity of the anterior CC was used to define the anteriormost division of the CC, indicating the genu. The rostral body was defined as the anterior one-third minus the genu. The anterior midbody was defined as the anterior half minus the anterior one-third. The posterior half included the posterior midbody, isthmus and splenium. The posterior midbody was defined as the posterior half minus the posterior one-third. The isthmus was defined as the posterior one-third minus the posterior one-fifth. The posteriormost one-fifth of the CC represented the splenium. Next, tracts of interest were calculated between two parasagittal planes located 3.8 mm (two planes) on either side of the midsagittal CC. Mean FA and MD for each voxel comprising each set of fibers were measured. Statistical analyses were performed using SPSS for Windows 11.0.1J software (SPSS, Japan Co., Tokyo, Japan). Initially, differences in FA and MD values of the CC subregions between MyD patients and healthy subjects were evaluated using Student's *t*-test. Values of  $p < 0.008$  ( $= 0.05/6$ ) were considered statistically significant to avoid type I errors in the multiplicity of statistical analysis. Relationships of the FA and MD values of CC subregions with CTG expansion, age at onset, age at scan date, and disease duration were evaluated using Pearson's correlation method. Values of  $p < 0.008$  ( $= 0.05/6$ ) were considered significant.

To clarify volume differences between patients and healthy subjects, structural 3D T1-weighted MR images were ana-

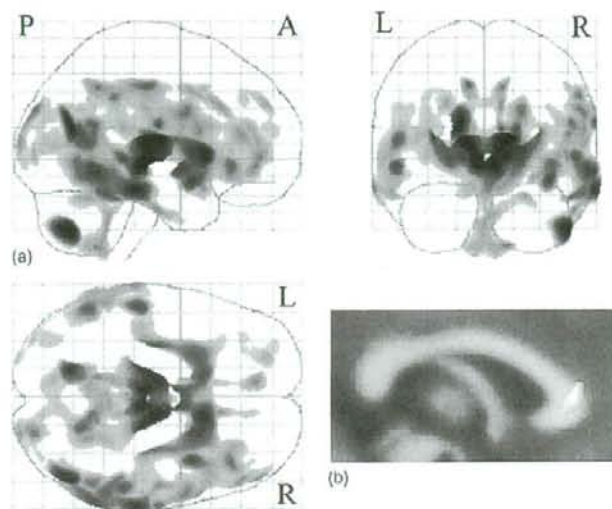


Fig. 1. (a) Regions of atrophy for gray matter in myotonic dystrophy patients compared to healthy subjects (two-sample *t*-test, SPM 2). Significant volume losses were detected in the prefrontal cortex, thalamus, striatum, temporal cortex and occipital cortex, but not in the parietal cortex. (b) Regions of atrophy for the corpus callosum in myotonic dystrophy patients compared to healthy subjects (two-sample *t*-test, SPM 2). Significant volume decrease was detected in the genu.

lyzed using an optimized VBM technique. Data were analyzed using Statistical Parametric Mapping 2 (SPM2) software (Wellcome Department of Imaging Neuroscience, London, UK) running on MATLAB 6.5 (Math Works, Natick, MA). Images were processed using optimized VBM script (dbm.neuro.uni-jena.de/vbm.html). Details of this process are described elsewhere [10]. Normalized segmented images were modulated by multiplication with Jacobian determinants of spatial normalization function to encode the deformation field for each subject as tissue density changes in normal space. Images were smoothed using a 12 mm full-width half-maximum of an isotropic Gaussian kernel. Statistical analyses were performed using SPM2 software. Differences in regional gray matter volume and white matter volume, especially callosal volume, between MyD patients and healthy subjects were assessed by the two-sample *t*-test, while the relationship between regional gray matter volume and CTG expansion, disease duration, age at onset, and age at scan date of the MyD patients was evaluated by single regression model. Only correlations that met these criteria were deemed statistically significant. In this case, a seed level of  $p < 0.001$  (uncorrected) and a cluster level of  $p < 0.05$  were selected.

Significant differences in FA and MD were noted between MyD patients and healthy subjects in the genu, rostral body, anterior midbody, posterior midbody and splenium (Table 1). Only the difference in FA in the splenium was at a trend level ( $p = 0.019$ ). No significant differences were noted in the isthmus. However, no correlations were found between FA and MD values and CTG expansion, disease duration, age at onset, and age at scan date in MyD patients (data not shown).

CC subregions comprised fibers connecting associated cortical regions, so atrophy of these areas was evaluated using VBM analysis. Significantly decreased volumes in prefrontal,

temporal and occipital areas, thalamus and striatum were found, but not in parietal areas (Fig. 1a), where connecting fibers pass through the isthmus. The callosal volume was also measured, with volume loss being detected only in the genu of CC subregions (Fig. 1b). Significant negative correlations were also found between cerebral volumes and CTG expansion in bilateral motor areas (Fig. 2). These areas were not correlated with disease duration, age at onset, or scan date (data not shown).

DTI was used to evaluate microstructural changes in CC subregions in 11 MyD patients. Changes in FA and MD values were detected in the genu, rostral body, anterior midbody, posterior midbody and splenium, comprising fibers connecting the frontal area, motor system, and temporal and occipital areas. No such changes were detected in the isthmus containing fibers connecting to the parietal area. Conversely, VBM analysis revealed regional volume atrophy of areas, such as the prefrontal cortex, thalamus, striatum, temporal cortex and occipital cortex, but not the parietal cortex. These changes in the microstructure of CC subregions corresponded well with atrophic cortical areas, where fibers connecting between the hemispheres ran through these CC subregions. This study also revealed that CTG expansion size correlates with volume loss of the motor and prefrontal cortices.

Only two previous studies have evaluated FA and MD changes of the brain in MyD patients, examining various white matter areas. Regarding the CC, only estimations of the genu and splenium were made, and those data were consistent with our own findings. However, no estimations of the rostral body, midbodies or isthmus were made [9,23]. Furthermore, data were obtained from manually plotted ROIs, whereas our data were obtained from 3D fiber tracts between the two parallel parasagittal planes on either side of the midsagittal CC.



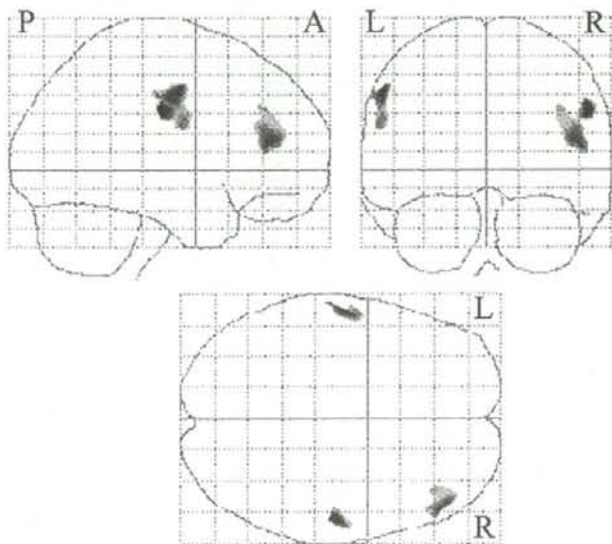


Fig. 2. Relationship between regional gray matter volume and CTG expansion in MyD patients (single regression model, SPM2). There was negative correlation between CTG expansion size and gray matter volumes of the bilateral motor area and right prefrontal cortex.

Our detailed examination showed differences in microstructural changes between the two sides.

No postmortem studies have revealed neuronal degeneration of the CC, but cortical neuronal losses are known to occur in gray matter of MyD patients [18]. These changes in CC may suggest that the loss of myelin and axonal membranes in some CC subregions may be due to Wallerian degeneration derived from atrophy of those projected cortical areas [19]. The absence of microstructural changes in the isthmus would be due to the lack of atrophic changes of the parietal cortex. The difference in FA at the splenium, which comprises fibers connecting temporal and occipital lobes, was at a trend level. In our study, regional volume losses were also revealed in temporal and occipital cortices. The failure to detect significant changes in the splenium could thus be ascribed to the degree of volume changes. In the occipital lobe, cortical atrophic changes were lower than in other cortical regions in our patients. To determine whether the changes of FA in CC subregions were related to CC subregion volume losses, we investigated the callosal volume. Significant volume decrease was shown only in the genu, not in the other CC subregions. This indicated that the reduction of callosal volume did not contribute to the reduction of anisotropy. Furthermore, it may suggest that the microstructural changes precede the morphometrical changes of the CC subregions.

Microstructural changes in the rostral body, anterior midbody and posterior midbody would be caused not only by degeneration of the frontal area, but also by dysfunction of the motor system. Decreases in volume of the thalamus and striatum were detected in this study, and neuropathological changes in the thalamus, caudate, brainstem nuclei and the so-called motor system are well known [6,11,20]. These changes were of major interest both for research and clinical practice. However, regarding

DTI analysis, the thalamus and striatum are known to display laterality and subregional differences [3,7], and comprehensive evaluation of the motor system is complicated. FA and MD values of these areas could thus serve as indices of disturbance across motor areas. The mean MD value in the isthmus of CC in normal subjects is larger than in other subregions. However, a previous study showed that the MD of the isthmus is larger and accelerated along with age compared to the other CC subregions, and the data of the present study corresponded well with the previous one [21].

In this study, correlations between DTI metrics and clinical features, such as age at scan and CTG repeat were not found. This may be due to the fact that the age distribution of MyD was quite narrow (one was 34 years old, and the others were 50–64 years old), and thus the results were not influenced by an aging effect. This VBM analysis showed a correlation between CTG repeat and the limited regional volumes. However, the FA and MD values of the CC subregions were indirect indices of the related cortical regions, and the slight changes of gray matter would not affect the FA and MD values of CC subregions.

Correlation between changes of brain structures and CTG expansion were analyzed, and it was revealed for the first time that CTG expansion size correlates with volume loss of the motor and prefrontal cortices. CTG expansion size is known to correlate with disease severity [11], cognitive executive (frontal) deficits [24], full scale intelligence quotient (IQ), performance IQ, and verbal IQ [15]. Motor areas in MyD patients were smaller than in healthy subjects [1]. Cerebral hypoperfusion of the frontal lobe and working memory deficit were also reported in MyD patients [5,15]. Our findings may explain the correlations between these changes. Previous studies were unable to detect correlations between volume and CTG expansion size

Table 1  
Differences in fractional anisotropy (FA) and mean diffusivity (MD) in myotonic dystrophy (MyD) patients and healthy subjects

	Genus	RB	AMB	PMB	Isthmus	Splenium
FA in MyD patients	0.70 ± 0.09 ( <i>r</i> = 4.56)	0.56 ± 0.07 ( <i>r</i> = 3.45)	0.60 ± 0.10 ( <i>r</i> = 3.15)	0.61 ± 0.11 ( <i>r</i> = 3.42)	0.61 ± 0.08 ( <i>r</i> = 1.43)	0.77 ± 0.07 ( <i>r</i> = 2.73)
FA in healthy subjects	0.84 ± 0.04	0.70 ± 0.12	0.72 ± 0.09	0.74 ± 0.08	0.66 ± 0.10	0.84 ± 0.04
MD in MyD patients	10.27 ± 1.85 ( <i>r</i> = -5.13)	11.45 ± 1.92 ( <i>r</i> = -3.49)	10.82 ± 2.79 ( <i>r</i> = -2.93)	10.73 ± 1.42 ( <i>r</i> = -4.78)	11.36 ± 2.06 ( <i>r</i> = -2.04)	9.00 ± 1.10 ( <i>r</i> = -4.02)
MD in healthy subjects	7.23 ± 0.73	8.62 ± 2.06	8.38 ± 1.04	8.46 ± 0.88	9.92 ± 1.38	7.46 ± 0.78

RB: Rostral body; AMB: anterior midbody; PMB: posterior midbody; MD: ( $10^{-4}$  mm<sup>2</sup>/s).

\* Significant difference between MyD patients and healthy subjects;  $p < 0.008$  ( $= 0.05/6$ ) was considered significant.

\*\* Difference between MyD patients and healthy subjects at a trend level ( $p < 0.05$ ).

[1]. Participants in those studies contained patients who became ill in childhood. Patients with early onset, such as congenital MyD are known to show severe neuromuscular symptoms and CNS disorders [11]. A combination of adult and younger onset patients may thus affect the results. However, the number of patients in the present study was small, raising the question of adequate statistical power. Further studies with larger groups of patients and controls are warranted to confirm our results.

In summary, microstructural changes of FA and MD in CC subregions connecting to cortical areas correlate well with cortical volumes in MyD patients. Significant negative correlations also exist between the volume of the frontal cortex, particularly the bilateral motor areas, and CTG triplet expansion size. DTI and VBM demonstrated the presence of microstructural changes, especially in motor neurons of MyD patients.

## References

- [1] G. Antonini, C. Mainero, A. Romano, F. Giubilei, V. Ceschin, F. Gragnani, S. Morino, M. Fiorelli, F. Soscia, A. Di Pasquale, F. Caramia, Cerebral atrophy in myotonic dystrophy: a voxel based morphometric study, *J. Neurol. Neurosurg. Psychiatry* 75 (2004) 1611–1613.
- [2] P.J. Basser, C. Pierpaoli, Microstructural and physiological features of tissue elucidated by quantitative diffusion-tensor MRI, *J. Magn. Res. B* 111 (1996) 209–219.
- [3] T.E. Behrens, H. Johansen-Berg, M.W. Woolrich, S.M. Smith, C.A. Wheeler-Kingshott, P.A. Boulby, G.J. Barker, E.L. Sillery, K. Sheehan, O. Ciccarelli, A.J. Thompson, J.M. Brady, P.M. Matthews, Non-invasive mapping of connections between human thalamus and cortex using diffusion imaging, *Nat. Neurosci.* 6 (2003) 750–757.
- [4] B. Censori, L. Provinciali, M. Danni, L. Chiaramoni, M. Maricotti, N. Foschi, M. Del Pesce, U. Salvolini, Brain involvement in myotonic dystrophy: MRI features and their relationship to clinical and cognitive conditions, *Acta Neurol. Scand.* 90 (1994) 211–217.
- [5] L. Chang, T. Anderson, O.A. Migneco, K. Boone, C.M. Mehlinger, J. Villanueva-Meyer, N. Berman, I. Mena, Cerebral abnormalities in myotonic dystrophy. Cerebral blood flow, magnetic resonance imaging, and neuropsychological tests, *Arch. Neurol.* 50 (1993) 917–923.
- [6] A. Culebras, R.G. Feldman, F.B. Merk, Cytoplasmic inclusion bodies within neurons of the thalamus in myotonic dystrophy. A light and electron microscope study, *J. Neurol. Sci.* 19 (1973) 319–329.
- [7] A.J. Fabiano, M.A. Horsfield, R. Bakshi, Interhemispheric asymmetry of brain diffusivity in normal individuals: a diffusion-weighted MR imaging study, *Am. J. Neuroradiol.* 26 (2005) 1089–1094.
- [8] Y.H. Fu, A. Pizzuti, R.G. Fenwick Jr., J. King, S. Rajnarayan, P.W. Dunne, J. Dubel, G.A. Nasser, T. Ashizawa, P. DeJong, B. Wieringa, R. Korneluk, B.M. Perryman, H.F. Epstein, C.T. Caskey, An unstable triplet repeat in a gene related to myotonic dystrophy, *Science* 255 (1992) 1256–1258.
- [9] H. Fukuda, J. Horiguchi, C. Ono, T. Ohshita, J. Takaba, K. Ito, Diffusion tensor imaging of cerebral white matter in patients with myotonic dystrophy, *Acta Radiol.* 46 (2005) 104–109.
- [10] C.D. Good, I. Johnsrude, J. Ashburner, R.N.A. Henson, K.J. Friston, R.S.J. Frackowiak, Cerebral asymmetry and the effect of sex and handedness on brain structure: a voxel-based morphometric analysis of 465 normal adult human brains, *Neuroimage* 14 (2001) 685–700.
- [11] P.S. Harper, *Myotonic Dystrophy, Major Problems in Neurology*, vol. 37, third ed., W.B. Saunders, London, 2001, pp. 139–165.
- [12] K.M. Hasan, R.K. Gupta, R.M. Santos, J.S. Wolinsky, P.A. Narayana, Diffusion tensor fractional anisotropy of the normal-appearing seven segments of the corpus callosum in healthy adults and relapsing-remitting multiple sclerosis patients, *J. Magn. Reson. Imag.* 21 (2005) 735–743.
- [13] H. Huang, J. Zhang, H. Jiang, S. Wakana, L. Poetscher, M.I. Miller, P.C.M. van Zijl, A.E. Hillis, R. Wytko, S. Mori, DTI tractography based parcellation of white matter: application of the mid-sagittal morphology of corpus callosum, *Neuroimage* 26 (2005) 295–305.

- [14] S. Hunsche, M.E. Moseley, P. Stoeter, M. Hedehus, Diffusion tensor MR imaging at 1.5 and 3.0 T: initial observations, *Radiology* 221 (2001) 550–556.
- [15] E. Kato, S. Takahashi, H. Yonezawa, Intellectual impairment and brain MRI findings in myotonic dystrophy: with a special reference to hippocampal atrophy and white matter lesions, *Rinsho Shinkeigaku* 35 (1995) 859–864.
- [16] D. Le Bihan, Molecular diffusion, tissue microdynamics and microstructure, *NMR Biomed.* 8 (1995) 375–386.
- [17] D. Le Bihan, Looking into the functional architecture of the brain with diffusion MRI, *Nat. Rev. Neurosci.* 4 (2003) 469–480.
- [18] K. Mizukami, M. Sasaki, A. Baba, T. Suzuki, H. Shiraishi, An autopsy case of myotonic dystrophy with mental disorders and various neuropathologic features, *Psychiatry Clin. Neurosci.* 53 (1999) 51–55.
- [19] T. Ogawa, Y. Yoshida, T. Okudera, K. Noguchi, H. Kado, K. Uemura, Secondary thalamic degeneration after cerebral infarction in the middle cerebral artery distribution: evaluation with MRI imaging, *Radiology* 204 (1997) 255–262.
- [20] S. Ono, K. Inoue, T. Mannen, F. Kanda, K. Jinnai, K. Takahashi, Neuropathological changes of the brain in myotonic dystrophy – some new observations, *J. Neurol. Sci.* 81 (1987) 301–320.
- [21] M. Ota, T. Obata, Y. Akine, H. Ito, H. Hiroo, T. Asada, T. Suhara, Age-related degeneration of corpus callosum measured with diffusion tensor imaging, *Neuroimage* 31 (2006) 1445–1452.
- [22] C. Pierpaoli, P.J. Basser, Toward a quantitative assessment of diffusion anisotropy, *Magn. Res. Med.* 36 (1996) 893–906.
- [23] J. Takaba, N. Abe, H. Fukuda, Evaluation of brain in myotonic dystrophy using diffusion tensor MR imaging, *Nippon Hoshasen Gijutsu Gakkai Zasshi* 59 (2003) 831–838.
- [24] S. Winblad, C. Lindberg, S. Hansen, Cognitive deficits and CTG repeat expansion size in classical myotonic dystrophy type 1 (DM1), *Behav. Brain Funct.* 15 (2006) 16.
- [25] S.F. Witelson, Hand and sex differences in the isthmus and genu of the human corpus callosum, *Brain* 112 (1989) 799–835.

# Functional interactions between entorhinal cortex and posterior cingulate cortex at the very early stage of Alzheimer's disease using brain perfusion single-photon emission computed tomography

Kentaro Hirao<sup>a,d</sup>, Takashi Ohnishi<sup>a</sup>, Hiroshi Matsuda<sup>a,b</sup>, Kiyotaka Nemoto<sup>a,c</sup>, Yoko Hirata<sup>a</sup>, Fumio Yamashita<sup>c</sup>, Takashi Asada<sup>c</sup> and Toshihiko Iwamoto<sup>d</sup>

**Objective** The cause of the reduced regional cerebral blood flow (rCBF) in the posterior cingulate cortex in the early stage of Alzheimer's disease has not been clarified. In Alzheimer's disease, the posterior cingulate cortex itself shows little neuropathologic degeneration, and a hypothesis explaining such a discrepancy is that the functional impairment in the posterior cingulate cortex reflects remote effects caused by degeneration in distant but connected areas, such as the entorhinal cortex. To test the hypothesis, we investigated the functional connectivity between the entorhinal cortex and posterior cingulate cortex.

**Methods** Sixty-one patients with probable Alzheimer's disease at a very early stage and 61 age-matched healthy controls underwent both brain structural magnetic resonance imaging (MRI) and single-photon emission computed tomography (SPECT). Voxel-based morphometry was performed on MRI data to identify clusters of significantly reduced grey matter concentration in patients with Alzheimer's disease relative to controls, which were set as volumes of interest (VOIs) for correlation analyses of SPECT images. We then used adjusted rCBF values in the VOIs as covariates of interest in statistical parametric mapping.

**Results** Voxel-based morphometry demonstrated a significant reduction in grey matter concentration in the bilateral entorhinal cortex in Alzheimer's disease. A positive correlation between rCBF in the entorhinal cortex as VOI and that in the limbic and paralimbic systems, including the

posterior cingulate cortex, anterior cingulate cortex, lingual gyri and left middle temporal gyrus ( $P < 0.001$ ), was observed in Alzheimer's disease. Control subjects also showed a similar correlation in the limbic and paralimbic systems, but not in the posterior cingulate cortex.

**Conclusion** These results indicate that rCBF changes in the posterior cingulate cortex may be closely related to those in the entorhinal cortex in patients with Alzheimer's disease, thereby supporting the 'remote effect' hypothesis. *Nucl Med Commun* 27:151-156 © 2006 Lippincott Williams & Wilkins.

*Nuclear Medicine Communications* 2006, 27:151-156

**Keywords:** Alzheimer's disease, mild cognitive impairment, regional cerebral blood flow, SPECT

<sup>a</sup>Department of Radiology, National Center Hospital for Mental, Nervous and Muscular Disorders, National Center of Neurology and Psychiatry, Tokyo, <sup>b</sup>Department of Nuclear Medicine, Saitama Medical School Hospital, Saitama, <sup>c</sup>Department of Neuropsychiatry, Institute of Clinical Medicine, University of Tsukuba, Tsukuba and <sup>d</sup>Department of Geriatric Medicine, Tokyo Medical University, Tokyo, Japan.

Correspondence to Hiroshi Matsuda MD, Department of Nuclear Medicine, Saitama Medical School Hospital, 38, Morohongo, Moroyama-machi, Iruma-gun, Saitama, 350-0495, Japan.  
Tel: +81 49 276 1302; fax: +81 49 276 1301;  
e-mail: matsudah@saitama-med.ac.jp

**Sponsorship:** This study was supported by the Promotion of Fundamental Studies in Health Science of the Organization for Pharmaceuticals and Medical Devices Agency.

Received 7 September 2005 Accepted 24 October 2005

## Introduction

Alzheimer's disease is a neurodegenerative disorder leading to amnesia, cognitive impairment and dementia, and is associated with pathological neuronal changes resulting from the accumulation of  $\beta$ -amyloid plaques and neurofibrillary degeneration (NFD) [1]. Delacourte *et al.* [2] reported that NFD with paired helical filaments tau was systematically present in varying amounts in the hippocampal region, not only in the very early stage of Alzheimer's disease, but also in non-demented aged subjects. When NFD was found in other brain areas, it

was always along a stereotypical, sequential, hierarchical pathway, and the progression was categorized into several stages according to the brain regions affected. According to this report, the posterior cingulate cortex is not affected by NFD at the early stage of Alzheimer's disease.

Morphological magnetic resonance imaging (MRI) studies have demonstrated that higher atrophy rates in the medial temporal regions, such as the entorhinal cortex and hippocampus, are observed in the very early stage of

Alzheimer's disease [3–6]. Moreover, recent advances in computer-assisted statistical imaging analysis have revealed that subjects with very mild Alzheimer's disease typically show abnormal metabolic and regional cerebral blood flow (rCBF) patterns even at the preclinical stage. Using glucose metabolism positron emission tomography (PET) with a voxel-by-voxel statistical analysis, Minoshima *et al.* [7] reported that the earliest changes observed in very mild Alzheimer's disease occur in the posterior cingulate cortex. This unexpected finding has been replicated by other groups using both glucose metabolism measurements with PET and less sophisticated measurement techniques, such as rCBF measurements with single-photon emission computed tomography (SPECT). Bradley *et al.* [8] reported that reduced perfusion appeared between the entorhinal and limbic stages pathologically defined by Braak and Braak [1] in the posterior cingulate cortex, as well as in the anterior temporal lobe, subcallosal area and precuneus. Our previous rCBF SPECT studies demonstrated significantly decreased rCBF in the posterior cingulate cortex and precuneus bilaterally in patients with mild cognitive impairment (MCI), proposed by Petersen *et al.* [9], when compared with controls at least 2 years before they satisfied a clinical diagnosis of Alzheimer's disease [10,11]. We also reported a diagnostic value of reduced rCBF in the posterior cingulate cortex to assist in discriminating between patients with probable Alzheimer's disease at the very early stage and age-matched controls before and after partial volume correction [12]. Furthermore, a PET study demonstrated hypometabolism of the posterior cingulate cortex in young subjects with a high genetic risk of developing Alzheimer's disease [13].

The fact that the posterior cingulate cortex itself shows little degeneration neuropathologically despite the significant reduction in its rCBF or glucose metabolism has been attributed to the possibility that the posterior cingulate cortex reflects remote effects caused by degeneration in distant but connected areas, such as the entorhinal cortex. In a non-human study, Baleyrier and Mauguier [14] reported that, in the monkey, the posterior cingulate cortex receives inputs from the parahippocampal gyrus, especially the entorhinal cortex, as well as from the subiculum and presubiculum. Furthermore, Meguro *et al.* [15] reported that lesions of the entorhinal cortex cause long-lasting, reduced cerebral glucose metabolism in the parietal, temporal and occipital associative cortices, posterior cingulate cortex and the hippocampal regions. Few in-vivo human studies on the functional connections between the entorhinal cortex and the rest of the brain, using neuroimaging techniques, have been published [16], although the association of atrophy of the medial temporal lobe with reduced rCBF in the posterior parietotemporal cortex has been reported

in patients with a clinical and pathological diagnosis of Alzheimer's disease [17].

In the present study, using MRI and SPECT, we examined the issue of whether functional connectivity exists between the posterior cingulate cortex and entorhinal cortex in humans, and whether the posterior cingulate cortex is subject to remote effects caused by degeneration in distant but connected areas, such as the entorhinal cortex, in the very early stage of Alzheimer's disease.

## Materials and methods

We studied retrospectively 61 patients (32 men and 29 women) with MCI who showed progressive cognitive decline and eventually fulfilled the diagnosis of probable Alzheimer's disease according to the National Institute of Neurological and Communicative Disorders and Stroke and the Alzheimer's Disease and Related Disorders Association (NINCDS-ADRDA) criteria [18] during the subsequent follow-up period of 2–6 years. They were recruited from 350 patients complaining of memory impairment in an Outpatient Memory Clinic at the National Center Hospital for Mental, Nervous and Muscular Disorders, National Center of Neurology and Psychiatry, Tokyo, Japan. They ranged in age from 48 to 87 years with a mean  $\pm$  standard deviation (SD) of  $70.6 \pm 8.4$  years. At the first visit, they showed selective impairment in delayed recall (more than 1.5 SD below the age-matched normal mean scores) of the word-list learning test, story recall test or Rey-Osterrieth complex test on neuropsychologic examination, without an apparent loss in general cognitive, behavioral or functional status. They corresponded to the MCI criteria and scored 0.5 in the Clinical Dementia Rating [19]. The Mini-Mental State Examination (MMSE) score [20] ranged from 24 to 29 (mean,  $26.0 \pm 1.5$ ) at the initial visit.

Sixty-one control subjects (30 men and 31 women; age, 54–86 years; mean,  $70.2 \pm 7.3$  years) were healthy volunteers without memory impairment or cognitive disorders. Specifically, their performance was within normal limits ( $< 1$ SD) on both the Wechsler Memory Scale-Revised and Wechsler Adult Intelligence Scale-Revised, and their MMSE score ranged from 26 to 30 (mean,  $28.7 \pm 1.5$ ). They did not differ significantly in age or education from the Alzheimer's disease patients. Spouses of the patients comprised the control subjects (not only spouses of the present patients but also spouses of other patients with advanced Alzheimer's disease). None of the control subjects manifested cognitive changes during the follow-up period of more than 2 years.

The local ethics committee approved the study for both healthy volunteers and patients with Alzheimer's disease, all of whom gave informed consent to participate. All

subjects were right-handed, were screened by questionnaire with regard to their medical history and were excluded if they had neurological, psychiatric or medical conditions that could potentially affect the central nervous system, such as substance abuse or dependence, atypical headache, head trauma with loss of consciousness, asymptomatic or symptomatic cerebral infarction detected by T2-weighted MRI, hypertension, chronic lung disease, kidney disease, chronic hepatic disease, cancer or diabetes mellitus.

All subjects underwent MRI and brain perfusion SPECT within 2 months after the first visit. The MRI data of a gapless series of thin sagittal sections were obtained using a three-dimensional volumetric acquisition of a T1-weighted MPRage sequence (1.0 T system; Magnetom Impact Expert; Siemens, Erlangen, Germany; echo time/repetition time, 4.4 ms/11.4 ms; flip angle, 15°; acquisition matrix, 256 × 256; one excitation; field of view, 31.5 cm; slice thickness, 1.23 mm). For the pretreatment of voxel-based morphometry (VBM) analysis of the two groups (patients with Alzheimer's disease and controls), image analysis was performed using Statistical Parametric Mapping 2 (SPM2; Wellcome Department of Cognitive Neurology, London, UK) running on MATLAB6.1 (Mathworks, Sherborn, Massachusetts, USA). Using SPM2 software, the original MRI images were first segmented by extraction of only grey matter, and the segmented images were spatially normalized into the standard space of Talairach and Tournoux [21]. Normalized images were then smoothed with a 12 mm full width at half-maximum isotropic Gaussian kernel to accommodate individual variability in the sulcal and gyral anatomy. The VBM analysis between patients with Alzheimer's disease and controls was performed by group analysis of SPM2 to identify clusters of significantly reduced grey matter concentration in patients with Alzheimer's disease relative to controls, which were set as volumes of interest (VOIs) for correlation analyses of SPECT images.

Before the SPECT scan was performed, all subjects had an intravenous line established. They were injected while lying supine with their eyes closed in a dimly lit quiet room. Each subject received an intravenous injection of 600 MBq of technetium-99m ethyl cysteinate dimer (<sup>99m</sup>Tc-ECD). Ten minutes after the injection of <sup>99m</sup>Tc-ECD, brain SPECT was performed using three-head rotating gamma cameras (Multispect3; Siemens Medical Systems, Inc., Hoffman Estates, Illinois, USA) equipped with high-resolution fan-beam collimators. For each camera, projection data were obtained in a 128 × 128 format for 24 angles at 50 s per angle. A Shepp and Logan Hanning filter was used for SPECT image reconstruction at 0.7 cycles/cm. Attenuation correction was performed using Chang's method. To calculate rCBF, the linearization algorithm of a curvilinear relationship between the

brain activity and blood flow was applied, as described in previous reports [22].

Partial volume correction was performed for atrophy correction in SPECT images using the above-mentioned three-dimensional volumetric T1-weighted magnetic resonance images, as described in previous studies [12,23]. In summary, partial volume correction was performed by dividing a grey matter SPECT image by a grey matter magnetic resonance image convoluted with equivalent spatial resolution to SPECT on a voxel-by-voxel basis. In the present study, a fully automated program for the partial volume correction, developed using C++ language, was employed.

The SPECT images after partial volume correction were analyzed with SPM2. Using a template for <sup>99m</sup>Tc-ECD, the SPECT data were transformed into a standard stereotaxic space. The spatial normalization algorithm of SPM2 was used for linear and non-linear transformation. A Gaussian filter (12 mm full width at half-maximum) was used to smooth each image. The effect of global differences in rCBF between scans was removed by proportional scaling with the threshold at 20% of whole brain activity. Using MRICro (<http://www.psychology.nottingham.ac.uk/staff/cr1/micro.html>), we checked the mask image for statistical analysis and verified that medial temporal regions, including the parahippocampal gyrus and hippocampus, were encompassed in the analysis. The rCBF values of the VOIs identified by VBM analysis in SPECT images after partial volume correction were extracted for each subject. The values were then adjusted using the equation,  $100 \times (\text{rCBF of VOI})/(\text{each global cerebral blood flow})$ , and were treated as covariates of interest. Intercorrelations between different brain regions were analyzed using SPM2 to investigate functional interactions according to Horowitz *et al.* [24].

## Results

The VBM analysis demonstrated significant reductions of grey matter concentration in the left (-16 -7 15, *x y z*; *Z* = 7.46) and right (18 -9 -16, *x y z*; *Z* = 7.45) entorhinal cortex in the very early stage of Alzheimer's disease compared with controls (*P* < 0.001, corrected for multiple comparisons, Fig. 1). These areas were set as VOIs (1.4 cm<sup>3</sup> for each hemisphere). We used the adjusted rCBF values in these entorhinal cortex VOIs as the covariates of interest for correlation analysis of rCBF SPECT. Adjusted rCBF values in the entorhinal cortex VOIs ranged from 42.3 to 142.1% (mean ± SD, 83.4 ± 17.6%) and from 67.4 to 112.2% (mean ± SD, 88.4 ± 10.5%) for patients with Alzheimer's disease and controls, respectively. Patients with Alzheimer's disease did not show a significant reduction in grey matter concentration in the posterior cingulate cortex compared with controls, even at a lenient threshold (*P* < 0.01).

Correlation analysis ( $P < 0.001$ , corrected for multiple comparisons) revealed positive correlations between rCBF values in the entorhinal cortex and those in the limbic and paralimbic systems, including the posterior cingulate cortex, anterior cingulate cortex, lingual gyri and left middle temporal gyri, in Alzheimer's disease. In contrast, control subjects showed positive correlations in the limbic and paralimbic systems, but not in the posterior cingulate cortex (Table 1, Fig. 2).

## Discussion

The VBM analysis demonstrated a significant reduction in grey matter concentration in the bilateral entorhinal cortex in the very early stage of Alzheimer's disease compared with controls. The entorhinal cortex is a well-known site in which pathological changes of Alzheimer's disease occur, even at a very early stage [25]. This result corresponds to previous VBM studies [3-6]. Therefore, we believe that the results of VBM analysis confirm that the profile of SPECT is suitable for the aim of our study: the investigation of the functional interaction between

Fig. 1

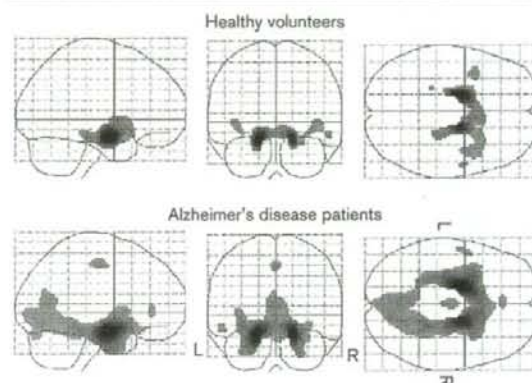


Orthogonal sections of Statistical Parametric Mapping 2 (SPM2) results for significant decline of grey matter concentration in patients with very early Alzheimer's disease compared with age-matched healthy volunteers ( $-16 -7 15$ ,  $x y z$ ;  $Z=7.46$ ;  $18 -9 -16$ ,  $x y z$ ;  $Z=7.45$ ). These regions correspond to bilateral Brodmann areas 34 (dorsal entorhinal cortex). Height threshold,  $<0.001$ ; corrected for multiple comparisons.

the rCBF in the entorhinal cortex and posterior cingulate cortex at the very early stage of Alzheimer's disease.

The more limited spatial resolution of SPECT scanners in comparison with PET does not allow an exact measurement of the local radiotracer concentration in brain tissue, as partial volume effects underestimate the activity in small structures of the brain. As focal brain atrophy accentuates the partial volume effect on SPECT measurements, actual rCBF values could be underestimated in the entorhinal cortex in Alzheimer's disease. To obtain accurate rCBF correlation between the entorhinal cortex and other brain areas, rCBF was

Fig. 2



Maximum intensity projections of Statistical Parametric Mapping 2 (SPM2) results for functional connectivities between the entorhinal cortex and the rest of the brain in healthy volunteers (top) and patients with Alzheimer's disease (bottom). Height threshold,  $<0.001$ ; corrected for multiple comparisons. Local maxima of regions of correlated regional cerebral blood flow (rCBF) are given in Table 1.

Table 1 Local maxima of brain areas in which regional cerebral blood flow (rCBF) is correlated with that in the entorhinal cortex

	Structure	Coordinates (mm)			Z-score
		x	y	z	
Healthy volunteers	Left amygdala	-18	-7	-15	Infinite
	Right amygdala	18	-5	-13	Infinite
	Right parahippocampal gyrus (BA35)	24	-26	-14	5.41
	Right superior temporal gyrus (BA21)	53	-2	-10	4.81
	Left insula	-40	10	0	4.8
	Left parahippocampal gyrus (BA36)	-22	-34	-10	4.5
Alzheimer's disease	Left amygdala	-18	-7	-15	Infinite
	Right amygdala	18	-3	-15	Infinite
	Right parahippocampal gyrus (BA36)	22	-36	-13	6.44
	Left parahippocampal gyrus (BA36)	-26	-34	-13	6.03
	Bilateral posterior cingulate cortex (BA23)	0	-63	14	5.66
	Right lingual gyrus (BA18)	12	-72	-3	5.62
	Bilateral dorsal posterior cingulate cortex (BA31)	0	-11	47	5.34
	Left lingual gyrus (BA18)	-4	-72	-3	5.12
	Left anterior cingulate cortex (BA24)	-4	37	0	4.85
	Left middle temporal gyrus (BA21)	-53	-1	-10	4.81

corrected for the partial volume effect in the present study. Although the correction for the partial volume effect has been reported to decrease the regional metabolic or rCBF difference between patients with Alzheimer's disease and control subjects [26], the decrease in intersubject variations of adjusted rCBF values has been reported to increase the statistical significance [12].

In the present study, correlation analysis showed positive correlations between rCBF values in the entorhinal cortex and in the limbic and paralimbic systems, including the posterior cingulate cortex, anterior cingulate cortex and lingual gyri, in Alzheimer's disease. In contrast, control subjects showed a correlation in the limbic and paralimbic systems, but not in the posterior cingulate cortex. Meguro *et al.* [15] reported that lesions of the entorhinal cortex in non-human primates cause a long-lasting reduced cerebral glucose metabolism in the hippocampus, the inferior parietal, posterior temporal and posterior cingulate cortex, and associative occipital cortices. Insausti *et al.* [27] also reported that the entorhinal cortex has connections to the limbic and paralimbic systems, including the anterior cingulate cortex and posterior cingulate cortex, insula in the temporal lobe, parainsula area in the parietal lobe, dorsolateral frontal cortex and an orbital region in the frontal lobe in the monkey. Our results in patients with Alzheimer's disease agreed well with these experimental results. With regard to control subjects, who showed similar correlations in the limbic and paralimbic systems, but not in the posterior cingulate cortex, Meguro *et al.* [15] have demonstrated that the degree of reduced cerebral glucose metabolism in areas that have connections with the entorhinal cortex correlates significantly with the severity of histologically determined damage in the entorhinal cortex. In Alzheimer's disease, the entorhinal cortex may be more markedly damaged than in controls, as adjusted rCBF values in the entorhinal cortex VOIs were approximately 6% lower on average in patients with Alzheimer's disease than in controls. Although our correlation analysis showed connections with the entorhinal cortex more strongly in patients with Alzheimer's disease than in controls, this may simply be due to a smaller range of adjusted rCBF values in the entorhinal cortex VOIs in controls than in patients with Alzheimer's disease. Although Mosconi *et al.* [16] reported the loss of entorhinal cortex correlations with cerebral cortices in glucose metabolism in patients with more advanced Alzheimer's disease, the entorhinal cortex correlation with the posterior cingulate cortex was observed in patients with Alzheimer's disease, but not in healthy control subjects, in a similar manner to the present study.

## Conclusion

According to an SPM approach to rCBF SPECT, we found enhanced functional connectivity between the entorhinal

cortex and posterior cingulate cortex in Alzheimer's disease at the very early stage. The results indicate that rCBF changes in the posterior cingulate cortex may positively correlate with those in the entorhinal cortex through this functional connectivity. Taken together, our results may support the existence of a 'remote effect'.

## Acknowledgements

We are very grateful to the technical staff of our hospital for the data acquisition of SPECT and MRI, and to Mr John Gelblum for proofreading the manuscript.

## References

- Braak H, Braak E. Neuropathological staging of Alzheimer-related changes. *Acta Neuropathol (Berl)* 1991; **82**:239-256.
- Delacourte A, David JP, Sergeant N, Buee L, Wattez A, Vermersch P, *et al.* The biochemical pathway of neurofibrillary degeneration in aging and Alzheimer's disease. *Neurology* 1999; **52**:1158-1165.
- Du AT, Schuff M, Amend D, Laakso MP, Hsu YY, Jagust WJ, *et al.* Magnetic resonance imaging of the entorhinal cortex and hippocampus in mild cognitive impairment and Alzheimer's disease. *J Neurol Neurosurg Psychiatry* 2001; **71**:441-447.
- Korf ES, Wahlund LO, Visser PJ, Scheitens P. Medial temporal lobe atrophy on MRI predicts dementia in patients with mild cognitive impairment. *Neurology* 2004; **63**:94-100.
- Nestor PJ, Scheitens P, Hodges JR. Advances in the early detection of Alzheimer's disease. *Nat Med* 2004; **10** (Suppl):S34-S41.
- Ohnishi T, Matsuda H, Tabira T, Asada T, Uno M. Changes in brain morphology in Alzheimer disease and normal aging: is Alzheimer disease an exaggerated aging process? *Am J Neuroradiol* 2001; **22**:1680-1685.
- Minoshima S, Giordani B, Berent S, Frey KA, Foster NL, Kuhl DE. Metabolic reduction in the posterior cingulate cortex in very early Alzheimer's disease. *Ann Neurol* 1997; **42**:85-94.
- Bradley KM, O'Sullivan VT, Soper ND, Nagy Z, King EM, Smith AD, *et al.* Cerebral perfusion SPET correlated with Braak pathological stage in Alzheimer's disease. *Brain* 2002; **125**:1772-1781.
- Petersen RC, Doody R, Kurz A, Mohs RC, Morris JC, Rabins PV, *et al.* Current concepts in mild cognitive impairment. *Arch Neurol* 2001; **58**:1985-1992.
- Kogure D, Matsuda H, Ohnishi T, Asada T, Uno M, Kunihiro T, *et al.* Longitudinal evaluation of early Alzheimer's disease using brain perfusion SPECT. *J Nucl Med* 2000; **41**:1155-1162.
- Imabayashi E, Matsuda H, Asada T, Ohnishi T, Sakamoto S, Nakano S, *et al.* Superiority of 3-dimensional stereotactic surface projection analysis over visual inspection in discrimination of patients with very early Alzheimer's disease from controls using brain perfusion SPECT. *J Nucl Med* 2004; **45**:1450-1457.
- Kanetaka H, Matsuda H, Asada T, Ohnishi T, Yamashita F, Imabayashi E, *et al.* Effects of partial volume correction on discrimination between very early Alzheimer's dementia and controls using brain perfusion SPECT. *Eur J Nucl Med Mol Imaging* 2004; **31**:975-980.
- Reiman EM, Chen K, Alexander GE, Caselli RJ, Bandy D, Osborne D, *et al.* Functional brain abnormalities in young adults at genetic risk for late-onset Alzheimer's dementia. *Proc Natl Acad Sci USA* 2004; **101**:284-289.
- Baleydier C, Manguiere F. The duality of the cingulate gyrus in monkey. Neuroanatomical study and functional hypothesis. *Brain* 1980; **103**:525-554.
- Meguro K, Blaizot X, Kondoh Y, Le Mestric C, Baron JC, Chavoix C. Neocortical and hippocampal glucose hypometabolism following neurotoxic lesions of the entorhinal and perirhinal cortices in the non-human primate as shown by PET. Implications for Alzheimer's disease. *Brain* 1999; **122**:1519-1531.
- Mosconi L, Pupi A, De Cristofaro MT, Fayyaz M, Sorbi S, Herholz K. Functional interactions of the entorhinal cortex: an 18F-FDG PET study on normal aging and Alzheimer's disease. *J Nucl Med* 2004; **45**:382-392.
- Jobst KA, Smith AD, Barker CS, Wear A, King EM, Smith A, *et al.* Association of atrophy of the medial temporal lobe with reduced blood flow in the posterior parietotemporal cortex in patients with a clinical and pathological diagnosis of Alzheimer's disease. *J Neurol Neurosurg Psychiatry* 1992; **55**:190-194.
- McKhann G, Drachman D, Folstein M, Katzman R, Price D, Stadlan EM. Clinical diagnosis of Alzheimer's disease: report of the NINCDS-ADRDA



- Work Group under the auspices of Department of Health and Human Services Task Force on Alzheimer's Disease. *Neurology* 1984; **34**: 939-944.
- 19 Hughes CP, Berg L, Danziger WL, Coben LA, Martin RL. A new clinical scale for the staging of dementia. *Br J Psychiatry* 1982; **140**:566-572.
  - 20 Folstein MF, Folstein SE, McHugh PR. 'Mini-mental state'. A practical method for grading the cognitive state of patients for the clinician. *J Psychiatr Res* 1975; **12**:189-198.
  - 21 Talairach J, Tournoux P. *Co-planar stereotaxic atlas of the human brain*. Stuttgart, New York: Thieme; 1988.
  - 22 Matsuda H, Yagishita A, Tsuji S, Hisada K. A quantitative approach to technetium-99m ethyl cysteinyl dimer: a comparison with technetium-99m hexamethylpropylene amine oxime. *Eur J Nucl Med* 1995; **22**: 633-637.
  - 23 Matsuda H, Ohnishi T, Asada T, Li ZJ, Kanetaka H, Imabayashi E, *et al*. Correction for partial-volume effects on brain perfusion SPECT in healthy men. *J Nucl Med* 2003; **44**:1243-1252.
  - 24 Horowitz B, Duara R, Rapoport SI. Intercorrelations of glucose metabolic rates between brain regions: application to healthy males in a state of reduced sensory input. *J Cereb Blood Flow Metab* 1984; **4**:484-499.
  - 25 Gomez-Isla T, Price JL, McKeel Jr DW, Morris JC, Growdon JH, Hyman BT. Profound loss of layer II entorhinal cortex neurons occurs in very mild Alzheimer's disease. *J Neurosci* 1996; **16**:4491-4500.
  - 26 Ibanez V, Pietrini P, Alexander GE, Furey ML, Teichberg D, Rajapakse JC, *et al*. Regional glucose metabolic abnormalities are not the result of atrophy in Alzheimer's disease. *Neurology* 1998; **50**:1585-1593.
  - 27 Insausti R, Amaral DG, Cowan WM. The entorhinal cortex of the monkey: - II. Cortical afferents. *J Comp Neurol* 1987; **264**:356-395.



## Case report

## Efficacy of milnacipran on the depressive state in patients with Alzheimer's disease

Katsuyoshi Mizukami<sup>a,\*</sup>, Yoshiro Tanaka<sup>b</sup>, Takashi Asada<sup>a</sup><sup>a</sup> Department of Psychiatry, Institute of Clinical Medicine University of Tsukuba, Japan, 1-1-1 Tennodai, Tsukuba City, Ibaraki 305-8575, Japan<sup>b</sup> Department of Psychiatry, Ishizaki Hospital, Kami-Ishizaki 4698, Ibaraki-machi, Higashi Ibaraki-gun, Ibaraki 311-3122, Japan

Available online 17 April 2006

## Abstract

An open-labeled study was conducted to examine the efficacy of selective serotonin and noradrenaline reuptake inhibitor (SNRI), milnacipran in treating depression in Alzheimer's disease (AD) patients. Eleven patients with AD showing major depressive symptoms were examined. Ten of 11 patients demonstrated an over 50% decrease in their HAM-D scores from the baseline, and 8 of 11 patients reached remission (HAM-D score  $\leq 7$ ) within 12 weeks of the start of milnacipran treatment, and their GAF score was also remarkably improved. Although in 11 patients, two patients showed a mild hypomanic state and one patient showed daytime somnolence, these problems were quickly solved after a decrease in the daily dose or discontinuation of milnacipran. In addition, the treatment had no negative effects on cognitive function of the patients. Our study results suggest that milnacipran is a promising medicine for depressive state in AD patients.

© 2006 Elsevier Inc. All rights reserved.

Keywords: Alzheimer's disease; Depression; Milnacipran; SNRI; SSRI

## 1. Introduction

In Alzheimer's disease (AD) patients, depression is not a rare condition. The prevalence of major depression has been reported to be within the range of 20–25% (Migliorelli et al., 1994; Olin et al., 2002) of AD patients. Depression in AD patients is associated with earlier placement out of the community into a nursing home (Steele et al., 1990), and is also associated with greater impairments in the quality of life (Gonzales-Salvador et al., 2000) as well as with increased caregiver depression and burden (Gonzales-Salvador et al., 1999). Although some tricyclic anti-depressants (TCAs) have been found to improve depression in AD, the anti-cholinergic effects of these medicines are critical to cognitive function in

AD patients (Teri et al., 1991). Recently, serotonin selective reuptake inhibitors (SSRIs) have been recommended for depression in AD patients due to their minimal anti-cholinergic effects, although their efficacy has remained controversial and further studies are needed.

Milnacipran (1-phenyl-1-diethyl-aminocarbonyl-2-amino-methyl-cyclopropane hydrochloride) is a novel anti-depressant agent that is a selective serotonin and noradrenaline reuptake inhibitor (SNRI) (Puech et al., 1997; Briley, 1998), and is reported to be devoid of any postsynaptic activity (Moret et al., 1985). Although milnacipran has been reported to be effective and safe for elderly depressive patients (Tignol et al., 1988), thus far there has been no study focusing on its effects on depression in AD patients. We describe here the efficacy and safety of milnacipran on depression with AD through its open trial for 11 patients. To our knowledge, this is the first paper reporting SNRI treatment of depression in AD patients.

## 2. Methods

## 2.1. Patients

A consecutive series of 11 patients were enrolled in this study, and all 11 participants were recruited from the outpatient

Abbreviations: AD, Alzheimer's disease; CDR, clinical dementia rating; DSM-IV, Diagnostic and Statistical Manual of Mental Disorders, fourth edition; FAST, Functional assessment staging; GAF, General assessment of functioning; HAM-D, Hamilton Depression Score; MMSE, Mini-mental state examination; MRI, Magnetic resonance imaging; SNRI, Serotonin and noradrenaline reuptake inhibitor; SPECT, Single photon emission computerized tomography; SSRI, Serotonin selective reuptake inhibitors; TCAs, Tricyclic anti-depressants.

\* Corresponding author. Tel./fax: +81 29 853 3182.

E-mail address: [mizukami@md.tsukuba.ac.jp](mailto:mizukami@md.tsukuba.ac.jp) (K. Mizukami).

clinic of Ishizaki Hospital, and provided written informed consent for study participation. The study was carried out in accordance with the ethics and principles embodied in the Declaration of Helsinki of 1975. Clinical diagnosis of AD was made utilizing DSM-IV (American Psychiatric Association, 1994) and NINCDS/ADRDA (McKhann et al., 1984) criteria. In addition, all 11 patients were diagnosed to be consistent with major depressive episode according to DSM-IV criteria, and their Hamilton Depression Score-17 (HAM-D17) (Hamilton, 1960) scores were greater than 12. All patients in this study were able to understand the contents of the interview and to describe their mental conditions.

### 2.2. Patient assessment

Patients also underwent physical, neurological, and routine laboratory examinations as well as brain magnetic resonance imaging (MRI). Patients were evaluated for cognitive and social function using the mini-mental state examination (MMSE) (Folstein et al., 1975), general assessment of functioning (GAF) according to DSM-IV, functional assessment staging (FAST) (Reisberg, 1988), and stage of the clinical dementia rating (CDR) (Hughes et al., 1982).

### 2.3. Drug administration

For 11 patients, treatment with milnacipran was begun after all evaluations were done. Seven patients started with milnacipran at 30 mg daily and 4 patients started with 15 mg daily. If patient showed no improvement for two weeks, the dose was increased by 15 mg/day. The participants underwent repeated evaluation for depressive states using the HAM-D every 2 weeks. Cognitive function using MMSE and social function using the GAF were also evaluated every 4 weeks. The average scores of HAM-D, MMSE, and GAF were compared between the baseline and the endpoint, which was defined as the time of 12 weeks after the start of milnacipran treatment. If patients discontinued milnacipran before 12 weeks, the week of the discontinuation was defined as the endpoint. A HAM-D score of 7 or below was defined as remission. Statistical analysis was carried out using the Wilcoxon method.  $p < 0.05$  is regarded as a significant difference.

## 3. Results

Eight patients took milnacipran for more than 12 weeks (72.7%); and 3 patients discontinued the treatment within 12 weeks. The reasons for discontinuation were emergence of hypomanic state for one patient (Case 5) and dropout for two patients (Cases 9 and 10). Case 10, however, resumed the treatment of milnacipran due to recurrence of depression thereafter.

Table 1 shows the background characteristics of the 11 patients analyzed. Their mean age was  $75.2 \pm 9.4$  (range 56–84) years. Of the 11 patients, 9 (81.8%) were female. The numbers of subjects for CDR 1 and CDR 2 ratings were 6 and 5, respectively, and the numbers of subjects for FAST 4, 5, and 6 stages were 8, 2, and 1, respectively. The average HAM-D,

Table 1  
Demographic characteristics of 11 patients

Variable		<i>p</i> value
Age (y, mean $\pm$ SD) (range)	75.2 $\pm$ 9.4 (56–84)	
Sex		
Male	2	
Female	9	
CDR		
1	6	
2	5	
FAST		
4	8	
5	2	
6	1	
HAM-D (mean $\pm$ SD) <sup>a</sup>		
Baseline	19.8 $\pm$ 3.7 (14–26)	
Endpoint	6.3 $\pm$ 3.8 (2–14)	<i>p</i> = 0.0030
GAF (mean $\pm$ SD) <sup>a</sup>		
Baseline	33.4 $\pm$ 12.6 (21–65)	
Endpoint	56.0 $\pm$ 11.8 (30–75)	<i>p</i> = 0.0032
MMSE (mean $\pm$ SD)		
Baseline	19.1 $\pm$ 4.2 (9–23)	
Endpoint	20.0 $\pm$ 4.7 (9–24)	<i>p</i> = 0.5368

<sup>a</sup> Significant.

MMSE, GAF scores of the 11 patients at baseline were  $19.8 \pm 3.7$  (range 14–26),  $19.1 \pm 4.2$  (range 9–23), and  $33.4 \pm 12.6$  (range 21–65), respectively.

One of 11 patients (Case 3) had a past history of major depressive episode, while the other 10 had no history of psychiatric illness including depression. The maximum average dose of milnacipran within 12 weeks was  $41.4 \pm 20.4$  mg (range 15–75 mg). The endpoint of the average HAM-D and GAF scores of 11 patients were  $6.3 \pm 3.8$  (range 2–14) and  $56.0 \pm 11.8$  (range 30–75), respectively. There is a significant difference in the average HAM-D and GAF scores between the baseline and the endpoint (at 12th week) ( $p = 0.0030$ ,  $p = 0.0032$ , respectively). In contrast, there is no significant difference in the average MMSE scores of 11 patients between the baseline and the endpoint ( $p = 0.5368$ ). Within 12 weeks, all the 11 patients showed improvement of depressive states, and 10 of 11 patients (except for Case 4) exhibited more than 50% HAM-D score reduction compared with the baseline score (Table 2). In addition, 8 patients reached remission (HAM-D score  $\leq 7$ ) at endpoint (12 weeks) and 5 patients reached remission within 4 weeks (Fig. 1). Broad aspects of depressive states, including depressive mood, anxiety, and psychomotor retardation, were improved by the treatment with milnacipran. Adverse reactions were observed in three patients. Although two patients (Cases 5 and 8) showed a mild hypomanic state and one patient (Case 1) showed daytime somnolence, these problems were quickly solved after a decrease in the daily dose (Cases 1 and 8) or discontinuation (Case 5) of milnacipran. The summary of 11 cases was shown in Table 2.

### 3.1. Case reports

Case 1 is a 84-year-old man with a 5-year history of cognitive decline and a 1-year history of depressive state,

Table 2  
Summary of 11 patients

No.	Age	Sex	Milnacipran (mg/day)		HAM-D			GAF		MMSE		Side effect
			Initial	Maximum	Baseline	Endpoint	% Changes	Baseline	Endpoint	Baseline	Endpoint	
1	84	M	30	60	18	5	-72%	35	45	15	14	Drowsiness
2	78	F	30	50	24	12	-50%	21	55	22	21	
3	79	F	30	30	23	5	-78%	25	60	23	21	
4	79	F	15	30	26	14	-46%	35	50	22	20	
5	71	F	30	30	19	7(4W)	-63%	25	30(4W)	9	9	Hypomanic
6	81	F	15	15	18	6	-67%	45	55	17	18	
7	77	F	30	30	14	4	-71%	65	75	22	24	
8	79	F	15	60	19	2	-89%	31	61	22	24	Hypomanic
9	84	M	15	15	18	8(5W)	-56%	35	65(5W)	21	22	
10	59	F	30	60	16	4(10W)	-75%	25	55(10W)	18	21	
11	56	F	30	75	23	2	-91%	25	65	19	23	
			24.5±7.6	41.4±20.4	19.8±3.7	6.3±3.8		33.4±12.6	56.0±11.8	19.1±4.2	20.0±4.7	

including severe depressive mood and loss of interest and moderate suicidal ideas. His depressive states had persisted despite treatment with fluvoxamine. He was started on 30 mg daily of milnacipran, which was gradually dosed up. At 60 mg he felt sleepiness, which was resolved by reduction to 45 mg. He recovered from his depression within 12 weeks.

Case 5 is a 71-year-old woman with a 4-year history of cognitive decline and a 1-month history of depressive state, with moderate depressive mood, loss of interest, and anxiety. She started on milnacipran at 30 mg daily, then 2 weeks later dosed down to 15 mg, and 4 weeks later discontinued due to slight hypomania. At 4 weeks, her mood disorder had resolved.

Case 8 is a 79-year-old woman with a 2-year history of cognitive decline and a 1 month history of depression characterized by moderate depressive mood, loss of interest, feelings of guilt, and psychomotor retardation. She started on milnacipran at 15 mg/day and dosed up to 60 mg. Her depression remitted within 4 weeks. At 60 mg daily, she showed a transient hypomanic state, which was quickly resolved by dose-down to 45 mg daily.

Case 10 was a 59-year-old woman with a 2-year history of cognitive decline and a 2-month history of depression, including

moderate depressive mood, feelings of guilt, suicidal ideas, and anxiety. She was started on a daily dose of 30 mg milnacipran. Milnacipran at 60 mg daily put her depression into remission at 8 weeks. However, her 2-month discontinuation of milnacipran caused her depressive state to recur, and then resumption of 45 mg/day milnacipran again improved her depressive state.

#### 4. Discussion

In our study, all the 11 patients demonstrated a remarkable improvement in depression with milnacipran treatment. Within 12 weeks, 8 of 11 patients reached remission (remission rate, more than 70%). Previous studies on depressive state in AD patients treated with anti-depressants demonstrated that the remission rates using clomipramine and fluoxetine, respectively, are 82% (Petracca et al., 1996) and 47% (Petracca et al., 2001), and that the rate of 30% reduction in HAM-D scores using fluoxetine and amitriptyline is 64% and 50%, respectively (Taragano et al., 1997). Thus, our study using milnacipran appears to have attained a very high remission rate, although there are some limitations to compare the results of our study with the previous studies. In addition, the majority of our patients showed a quick response, and 5 of 11 patients reached remission within 4 weeks. Interestingly, milnacipran has been reported to alleviate the symptoms of post-stroke depression within 1–2 weeks (Kimura et al., 2002). In addition, the onset of action of milnacipran is faster than that of SSRIs such as fluvoxamine and paroxetine (Morishia and Arita, 2003). Collectively, it is reasonable to suppose that milnacipran is effective in treating major depression in AD patients, and its effects appear within a short time interval. In our patients, with the treatment of milnacipran, all the 11 patients showed a remarkable improvement in GAF score according to the improvement of their depressive state, suggesting that milnacipran also has a beneficial impact on social function in AD patients.

Some reports have pointed out the placebo effect in the treatment of depression in AD patients (Petracca et al., 1996, 2001). Also in our study, it is possible that the placebo effect contributed to the improvement of depressive states. However, the remission rate using placebo has been reported to be

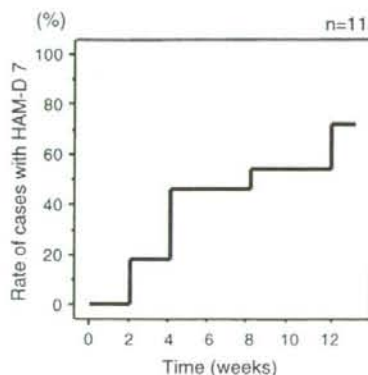


Fig. 1. Graph showing cumulative remission rate of 11 patients. Eight patients reached remission within 12 weeks, and 5 patients reached remission within 4 weeks.